

9. D. Banerjee, J. Lee, E.M. Dede, and H. Iizuka, Kilohertz magnetic field focusing in a pair of metallic periodic-ladder structures, *Appl Phys Lett* 99 (2011), 093501.
10. J. Lee, E.M. Dede, D. Banerjee, and H. Iizuka, Magnetic force enhancement in a linear actuator by air-gap magnetic field distribution optimization and design, *Finite Elem Anal Des* 58 (2012), 44–52.
11. E.M. Dede, J. Lee, Y. Guo, L.Q. Zhou, M. Zhang, and D. Banerjee, Kilohertz magnetic field focusing and force enhancement using a metallic loop array, *Appl Phys Lett* 101 (2012), 023506.
12. H. Tanaka and H. Iizuka, Kilohertz magnetic field focusing behavior of a single-defect loop array characterized by curl of the current distribution with delta function, *IEEE Antennas Wireless Propag Lett* 11 (2012), 1088–1091.
13. F. Gao, F. Zhang, M. Huang, and D.F. Sievenpiper, Programmable screen for patterning magnetic fields, *IEEE Trans Microwave Theory Tech* 62 (2014), 481–490.
14. H. Tanaka and H. Iizuka, Active control of magnetic field by manipulating induced currents in two-dimensional switch-mounted loop array, *IEEE Trans Magn* 49 (2013), 5682–5686.
15. FEKO user manual, Suite 6.1, EM software Systems-S.A. (Pty) Ltd, Stellenbosch, South Africa, 2011.
16. C.M. Butler, The equivalent radius of a narrow conducting strip, *IEEE Trans Antennas Propag* 30 (1982), 755–758.

© 2015 Wiley Periodicals, Inc.

## CIRCULARLY POLARIZED FREQUENCY RECONFIGURABLE KOCH ANTENNA FOR GSM/WI-FI APPLICATIONS

Venkateshwar V. Reddy and N. V. S. N. Sarma

Department of ECE, NIT, Warangal, Telangana, India; Corresponding author: vreddy2005@gmail.com

Received 4 May 2015

**ABSTRACT:** A novel circularly polarized frequency reconfigurable Koch fractal boundary antenna is proposed. Initially, a Koch slot is etched on the Koch fractal boundary patch of larger dimension ( $48 \times 48 \text{ mm}^2$ ). Within the etched slot, an asymmetrical Koch fractal patch of smaller dimension ( $36 \times 36 \text{ mm}^2$ ) is embedded and switches are introduced along x and y-directions to connect these inner and outer patch structures. By making ON/OFF switching of the diodes frequency reconfiguration is achieved. Measured results are in close agreement with the simulation results which demonstrates that the proposed antenna is well suited for GSM/Wi-Fi wireless applications. © 2015 Wiley Periodicals, Inc. *Microwave Opt Technol Lett* 57:2895–2898, 2015; View this article online at [wileyonlinelibrary.com](http://wileyonlinelibrary.com). DOI 10.1002/mop.29463

**Key words:** frequency reconfigurable; circular polarization; Koch fractal

### 1. INTRODUCTION

Rapid developments in the area of advanced wireless communication systems demand reconfigurable antennas. These antennas are divided into frequency, pattern, and polarization reconfigurable, based on the change of parameters in real time. Nowadays, all portable systems are supporting GSM/Wi-Fi services operating at different frequency bands. Instead of using multiple antennas for these applications, using a frequency reconfigurable antenna, the cost and space occupied on the system can be optimized. To avoid multipath signal fading effects and to make antenna orientation independent for signal reception, circularly polarized (CP) antennas are preferred. So, the design of single

probe feed CP, frequency reconfigurable antennas have become very attractive for modern day wireless communication systems.

Frequency reconfigurable antenna with defected ground structure and coplanar waveguide feeding technique is designed using diodes as switching elements on the radiating patch [1]. Microstrip slot antenna with switches in the slotted position is designed for frequency agility [2]. A frequency tunable antenna with loaded short circuited posts between the ground plane and slotted rectangular patch is discussed in [3] while the posts are placed at the patch edges. Capacitive loaded antenna with frequency reconfigurable ability is demonstrated in [4]. An L-shaped slot structure with PIN diodes, lumped capacitors and bias network is modeled for reconfigurable frequency [5], the diodes and capacitors are used at specific locations to create short circuits across the slot. A microstrip line fed inverted U-shaped antenna with diode and capacitor coupled slots is proposed for selective frequency reconfiguration [6]. However, most of the frequency reconfigurable antennas [1–6] in the open literature are based on microstrip line fed or CPW fed with diodes placed in the slotted section for linear polarization radiation. Moreover, it is because of the CPW feed and slotted ground plane structures these antennas are able to generate wide tuning range with broad impedance bandwidth. CP frequency reconfigurable slot antennas [7,8] are suggested by Row and coworkers. A multilayered single probe feed microstrip patch structure composed of conducting pins, varactor diodes, and capacitors is studied for frequency reconfigurable CP operation [9]. However, the fabrication complexity increases with stacked layers. In this work, frequency agility with single layer, single probe feed, and asymmetrical fractal boundary concept is examined for CP radiation at GSM and Wi-Fi wireless applications.

Fractal concept has been applied to design compact and multiband microstrip patch antennas. A microstrip line fed frequency tunable antenna with U-Koch slot and partial ground plane structure is studied by Ramadan et al. [10]. Fractal-based tree antennas are proposed to design miniaturized multiband as well as reconfigurable antennas [11]. Implementation of sierpinski monopole gasket with movable feed is investigated [12]. However, the reported fractal reconfigurable antennas [10–12] in the literature generate only linear polarization operation. Here, in this letter, using asymmetrical Koch fractal curves as boundaries of square patch, CP radiation is obtained. Such two asymmetrical Koch fractal patch structures connected with PIN diodes are examined for frequency reconfiguration at GSM (1.8 GHz) and ISM band (2.48 GHz) wireless applications.

### 2. ANTENNA DESIGN

Fractal curves are applied along boundaries of the conventional patch so that larger electrical lengths of antennas can be accommodated within a given space. Due to simple procedure in design, Koch curve has received lot of attention within fractal curve categories. Here, asymmetrical Koch fractal curves are used along boundaries of the patch to generate two orthogonal modes with equal amplitude for CP radiation [13,14]. The proposed Koch antenna indentation factor is indentation angle (IA). The nominated antenna side and top views are shown in Figure 1. A Koch fractal element with smaller dimension is inserted in the middle of the larger Koch. Outer Koch and inner Koch are connected with diodes ( $D_1$ ,  $D_2$ ,  $D_3$ , and  $D_4$ ) along x- and y-axis for switching operation. These switches permit the physical connection/disconnection of outer and inner fractal patch structures to change the antenna effective electrical length. In simulations, substrate of dielectric constant 2.2 with thickness 3.2 mm and

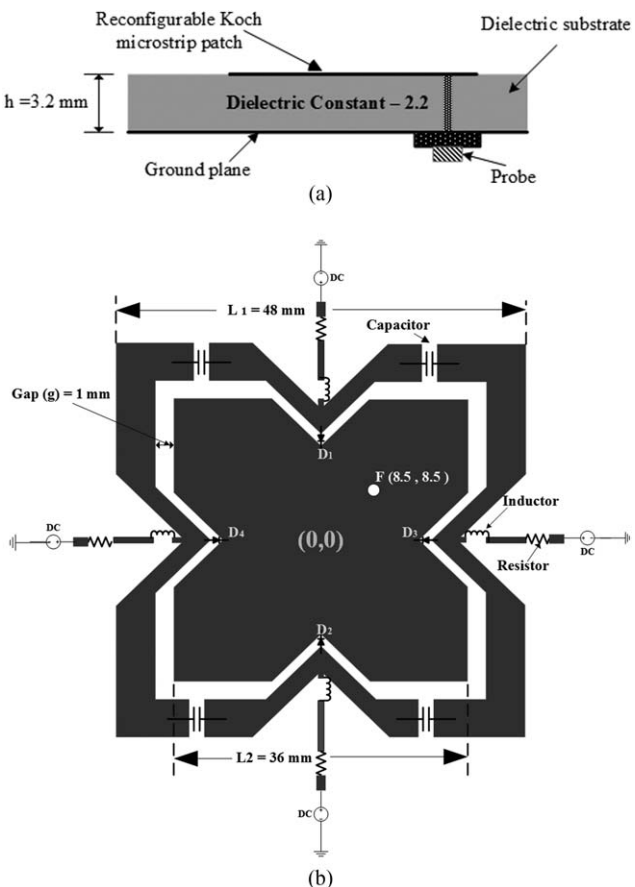


**Figure 1** Proposed frequency reconfigurable Koch antenna: (a) cross-sectional view and (b) top view

loss tangent 0.0019 is used. Perturbation to the structure for CP is inserted through edges; so that the coaxial line feed (*F*) point is fixed along the diagonal of the patch at (8.5 mm, 8.5 mm).

The studied patch structures are pictured in Figure 2. To facilitate better understanding of the proposed antennas frequency reconfiguration, the simulated current distributions on the Ant 1 at 2.48 GHz frequency and Ant 2 at 1.8 GHz frequency are shown in Figure 3. When all the switches are in OFF position, the frequency band at 2.48 GHz is mainly excited due to the strong current distribution along the fractal boundary curves of the inner patch as shown in Figure 3(a). As seen from Figure 3(b), the strong current distribution on the fractal curves of the outer patch excites 1.8 GHz resonance mode when all the switches are in ON position.

### 3. RESULTS AND DISCUSSION

Initially two individual linearly polarized square patch antennas are designed to operate at 1.8 and 2.48 GHz frequencies, respectively. The edges of these antennas are replaced with asymmetrical Koch fractal curves for CP radiation. Later, these two antennas are combined for frequency reconfigurable operation. The end to end lengths of outer and inner patch structures are considered as  $L_1 = 48$  mm and  $L_2 = 36$  mm, so that they can operate at GSM/Wi-Fi application bands. A gap of 1 mm is maintained between inner and outer patch to place diodes. The IAs of the fractal curves are optimized using the HFSS electromagnetic tool optometric analysis setup for good CP radiation. The outer fractal IAs ( $\theta_{x1}, \theta_{y1}$ ) and inner fractal IAs ( $\theta_{x2}, \theta_{y2}$ ) are optimized as (35°, 15°) and (45°, 20°), respectively. The

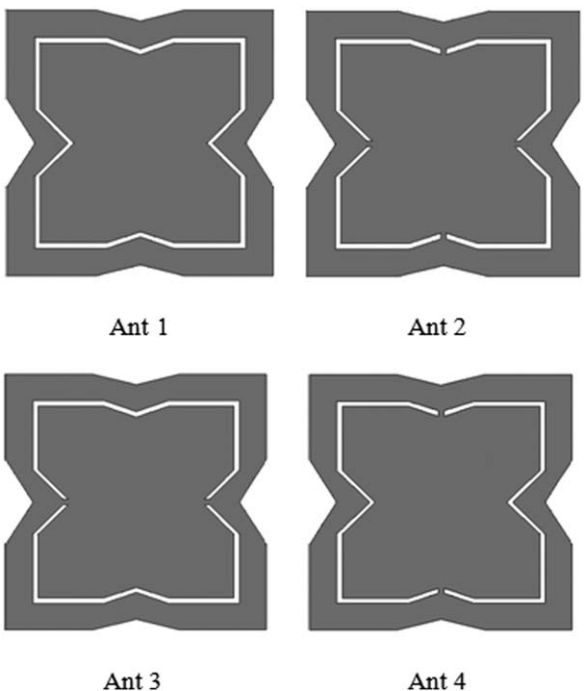


**Figure 2** The studied patch structures

outer and inner patch designs are connected with switches to generate CP frequency agile radiation. In the simulations, the behavior of the switch has been modeled using a microstrip line with the same scattering parameters of the PIN diode in both ON and OFF configurations.

By making the switches ON/OFF, different configurations are studied. In case of Ant 1, when all the switches are in OFF position, the outer fractal patch is isolated from inner patch thus leads to resonate only at 2.48 GHz frequency. When all the switches are in ON position Ant 2 resonates at only 1.8 GHz frequency. When the switches only along the *x*-axis (Ant 3) or only along the *y*-axis (Ant 4) are ON, antennas resonate at both the 1.8 and 2.48 GHz bands. By observing the Ant 3 and Ant 4 structures, it is understood that these antennas are having two isolated fractal curve slots on the patch with slot width 1 mm. These two Koch fractal slots are responsible for two resonating frequencies. The surface current distributions on the Ant 3 and Ant 4 at both the frequencies are pictured in Figure 4. The point to be observed is that for 1.8 GHz frequency the density of

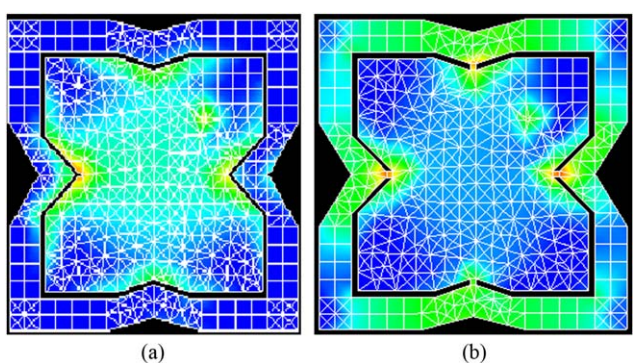


**Figure 3** The simulated current distributions: (a) Ant 1 at 2.48 GHz and (b) Ant 2 at 1.8 GHz. [Color figure can be viewed in the online issue, which is available at wileyonlinelibrary.com]

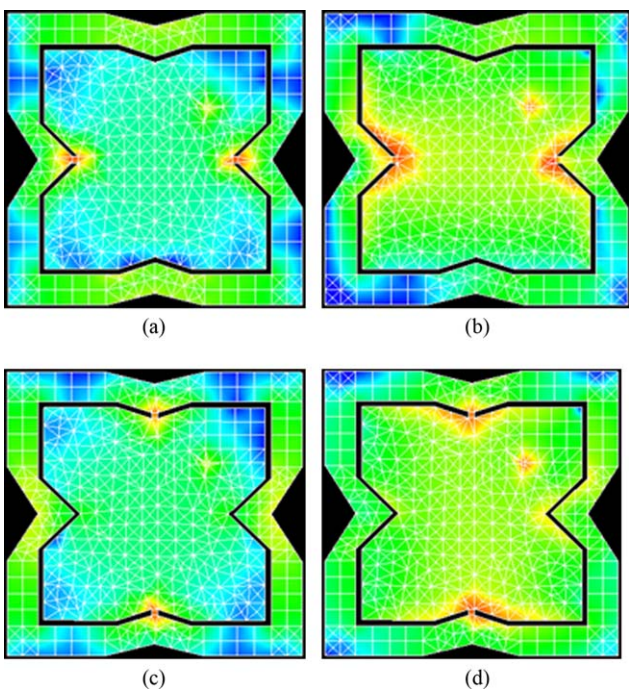


**Figure 4** The simulated surface current distributions on the patch Ant 3 and Ant 4. [Color figure can be viewed in the online issue, which is available at [wileyonlinelibrary.com](http://wileyonlinelibrary.com)]

current distribution is high along the outer fractal curves whereas it is high along the inner fractal curves for 2.48 GHz frequency. The simulated 10-dB return loss and 3-dB axial ratio (AR) bandwidths of Ant 1 are 2.8%, 1.3% and for Ant 2 are 4.2% and 1.8%, respectively.

To validate the simulations results, the proposed antenna is fabricated and experimentally studied. The fabricated antenna is pictured in Figure 5. The operation of the fabricated antenna is controlled using four PIN diode switches (MA4P789). To drive the switches, a direct bias voltage of 9 V is supplied to the diodes with thin traces of width 0.5 mm, the presence of which, as analyzed through electromagnetic simulations, does not disturb the radiation characteristics of the antenna. An inductor of 56 nH is used to block the RF from flowing in the DC supply trace, and a

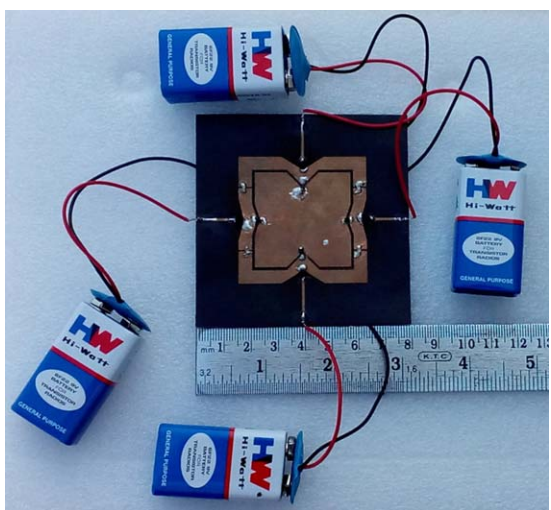


**Figure 5** The prototype of the fabricated antenna. [Color figure can be viewed in the online issue, which is available at [wileyonlinelibrary.com](http://wileyonlinelibrary.com)]

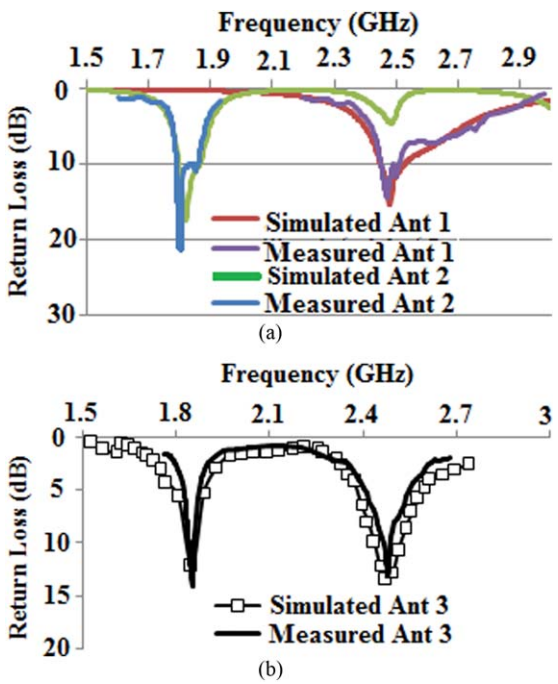


**Figure 6** The comparison of simulated and measured return loss results. [Color figure can be viewed in the online issue, which is available at [wileyonlinelibrary.com](http://wileyonlinelibrary.com)]

resistor of  $100\ \Omega$  is mounted to limit the voltage across the diode. A capacitor of value  $64\ \text{pF}$  is placed at proper locations of the outer patch to limit the DC bias voltage only to that particular diode; so that, it will not affect the adjacent diode ON/OFF condition. The comparison of the simulated and the measured results are portrayed in Figures 6–8. The deviations appearing between simulated and experimental results are due to tolerance levels during the fabrication process of the antenna.

The measured 10-dB return loss and 3-dB AR bandwidths of Ant 1 are 2.4% (2450–2510 MHz), 1.1% (2467–2493 MHz) and for Ant 2, 3.8% (1766–1834 MHz) and 1.6% (1786–1814 MHz), respectively. The measured 3-dB AR bandwidths of the Ant 3 at 1.8 GHz and 2.48 GHz frequencies are 1.2% and 0.9%, respectively. The measured radiation patterns of the Ant 1 and Ant 2 in the horizontal plane and vertical plane at 1.8 and 2.48 GHz are depicted in Figure 9. The antennas generate a gain of more than 3-dBi within operating frequency bands. So, by varying the IAs of

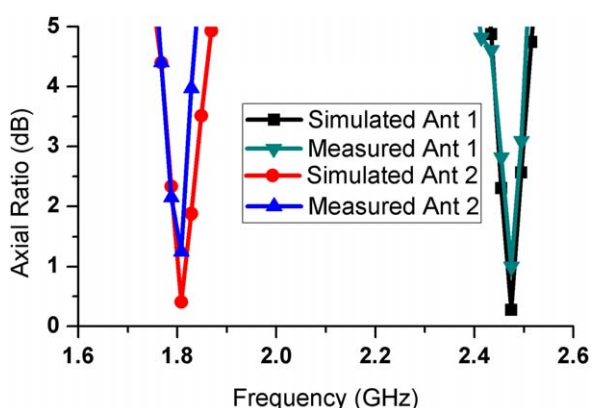


**Figure 7** The comparison of simulated and measured AR characteristics of Ant 1 and Ant 2. [Color figure can be viewed in the online issue, which is available at [wileyonlinelibrary.com](http://wileyonlinelibrary.com)]

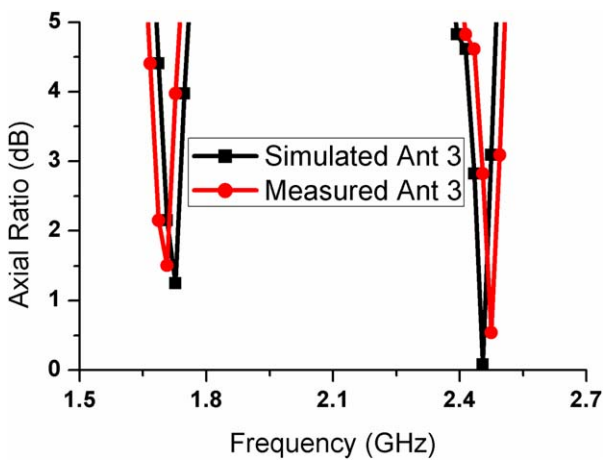


**Figure 8** The comparison of simulated and measured AR characteristics of Ant 3. [Color figure can be viewed in the online issue, which is available at [wileyonlinelibrary.com](http://wileyonlinelibrary.com)]

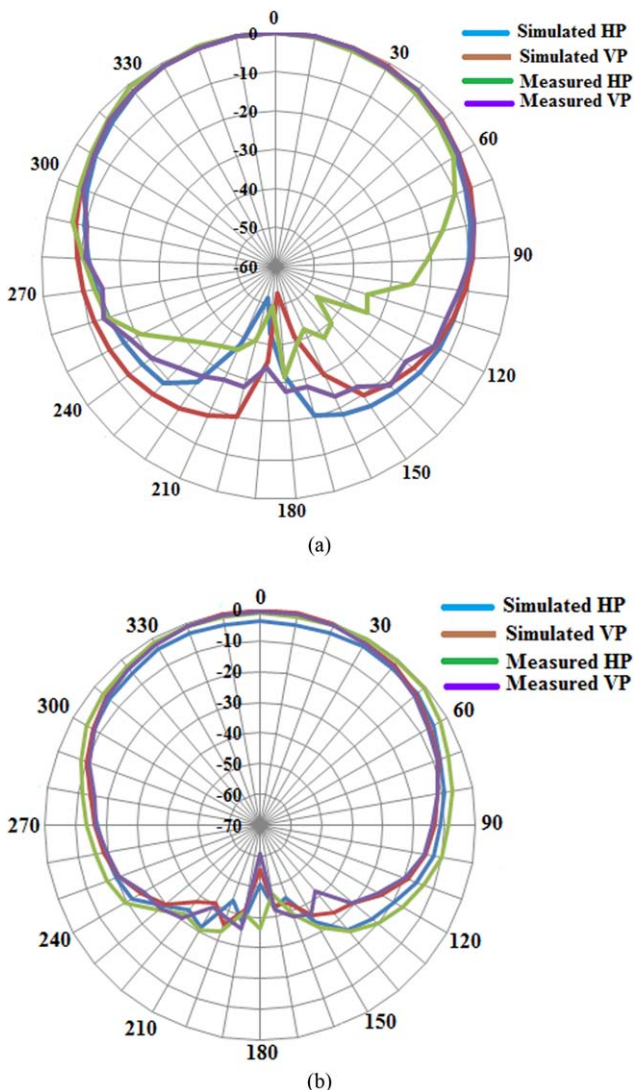


**Figure 9** The measured radiation patterns of Ant 1 and Ant 2. [Color figure can be viewed in the online issue, which is available at [wileyonlinelibrary.com](http://wileyonlinelibrary.com)]

the Koch fractal curves several frequency reconfigurable CP antennas at various applications can be designed. By replacing the Koch curves with Minkowski or T-type or poly fractal boundary curves several novel CP antennas for frequency reconfigurable operation can be attempted. Here, in the future designs by combining three, four, and so forth, asymmetrical patch structures and using diodes as switching elements, various multifunctional antennas working at different wireless applications can be attempted.

#### 4. CONCLUSION

A single probe feed CP frequency reconfigurable antenna using Koch fractal patch has been proposed and experimentally studied. The structure consists of two Koch patch designs; the smaller one is embedded in the middle portion of larger one. The dimensions of the patches are taken in such a way that they resonate at GSM (1.8 GHz) and Wi-Fi (2.48 GHz) frequencies. Asymmetrical Koch curves are used as boundaries of the two patches to generate CP. These patches are connected with PIN diodes. The obtained 3-dB AR bandwidths at GSM and Wi-Fi bands are 1.1% and 1.6%, respectively.

#### REFERENCES

1. H.B. El-Shaarawy, F. Coccetti, R. Plana, M. El-Said, and E.A. Hashish, Novel reconfigurable defected ground structure resonator on coplanar waveguide, *IEEE Trans Antennas Propag* 58 (2010), 3622–3628.
2. H.A. Majid, M.K.A. Rahim, M.R. Hamid, and M.F. Ismail, A compact frequency-reconfigurable narrowband microstrip slot antenna, *IEEE Antennas Wireless Propag Lett* 11 (2012), 616–619.
3. A.-F. Sheta and S.F. Mahmoud, A widely tunable compact patch antenna, *IEEE Antennas Wireless Propag Lett* 7 (2008), 40–43.
4. Y. Yu, J. Xiong, H. Li, and S. He, An electrically small frequency reconfigurable antenna with a wide tuning range, *IEEE Antennas Wireless Propag Lett* 10 (2011), 103–106.
5. M.I. Lai, T.Y. Wu, J.C. Hsieh, C.H. Wang, and S.K. Jeng, Design of reconfigurable antennas based on an L-shaped slot and PIN diodes for compact wireless devices, *IET Microwave Antennas Propag* 3 (2009), 47–54.
6. A. Mansoul, F. Ghanem, M.R. Hamid, and M. Trabelsi, A selective frequency-reconfigurable antenna for cognitive radio applications, *IEEE Antennas Wireless Propag Lett* 13 (2014), 515–518.
7. T.-Y. Lee and J.-S. Row, Frequency reconfigurable circularly polarized slot antennas with wide tuning range, *Microwave Opt Technol Lett* 53 (2011), 1501–1505.
8. C.C. Wang, L.T. Chen, and J.S. Row, Reconfigurable slot antennas with circular polarization, *Prog Electromagn Res Lett* 34 (2012), 101–110.
9. J.-S. Row and J.-F. Tsai, Frequency reconfigurable microstrip patch antennas with circular polarization, *IEEE Antennas Wireless Propag Lett* 13 (2014), 1112–1115.
10. A.H. Ramadan, K.Y. Kabalan, A. El-Hajj, S. Khoury, and S.M. Al-Husseini, A reconfigurable U-Koch microstrip antenna for wireless applications, *Prog Electromagn Res* 93 (2009), 355–367.
11. S.P. Joshua and D.H. Werner, Miniature reconfigurable three-dimensional fractal tree antennas, *IEEE Trans Antennas Propag* 52 (2004), 1945–1956.
12. M.M.A. Kumar, A. Patnaik, and C.G. Christodoulou, Design and testing of a multifrequency antenna with a reconfigurable feed, *IEEE Antennas Wireless Propag Lett* 13 (2014), 730–733.
13. P.N. Rao and N.V.S.N. Sarma, Minkowski fractal boundary single feed circularly polarized microstrip antenna, *Microwave Opt Technol Lett* 50 (2008), 2820–2824.
14. V.V. Reddy and N.V.S.N. Sarma, Compact circularly polarized asymmetrical fractal boundary microstrip antennas for wireless applications, *IEEE Antennas Wireless Propag Lett* 13 (2014), 118–121.